Online Minimum Switching Frequency Tracking Technique for Improving Reliability of IPOS Induction Heating Systems

Kyung-Wook Heo[1], Hyunjun Choi[2], and Jee-Hoon Jung[1]
[1] Electrical Engineering, Ulsan National Institute of Science and Technology, South Korea
[2] Korea Electronics Technology Institute, South Korea

***Abstract*-- This paper proposes an induction heating (IH) system structured by an input-parallel output-series (IPOS) for ship plate pre-heating. The proposed IH system provides a wide heating range for heating various ship plates using the IPOS structure. However, the impedance of the ship plate changes depending on the material, thickness, size, and temperature, which result in resonant frequency variations. It cannot guarantee the switching operation of the IH inverter in the inductive load region. Under the capacitive load region, the power switches fail their ZVS operation, and the system cannot linearly control power. In this paper, the minimum switching frequency tracking technique is proposed to improve the reliability of the IPOS IH heating system by guaranteeing the inductive region operation. A resonant frequency is estimated by using the impedance estimation of the resonant network. The validity of the proposed technique is experimentally verified using a 4-kW IPOS prototype IH system.**

***Index Terms*— Ship plate heating, IPOS IH system, Impedance estimation, ZVS capability.**

I. INTRODUCTION

Induction heating (IH) technology is gaining attention due to its advantages, such as a fast-heating, high efficiency, and clean heating [1]-[4]. Unlike the conventional heating method using fossil fuel, the IH system heats the object by the induced eddy currents, which are obtained by flowing high-frequency current through a working coil. IH does not generate by-products during heating compared with fossil fuels. The configuration of induction heating technology consists of a bridge circuit, a resonant network, and an IH coil [5]. As a bridge circuit used for induction heating, a half-bridge series resonant inverter (HB-SRI) is used because of its cost-effectiveness in the home application [6]-[8].

However, the above configuration cannot be used for the industry, which required rapid heating using a high-output power. The industry demands a method of rapidly increasing the temperature of the load by increasing the output power rather than user convenience. To obtain the high output power in the IH system, the output voltage applied to the resonant network should be increased. When the conventional full-bridge inverter is used, high-rated power switches are required, which increases the total system cost. In addition, it is difficult to design a system suitable for the various power required by the industry. It is not proper for mass production.

The resonant network must operate in an inductive load region to operate the IH system with high power conversion efficiency. When the power switches operate under the capacitive load region, ZVS cannot be achieved as the resonant current does not conduct the reverse diode of the power switch during dead time. It not only leads to the low power conversion efficiency of the entire system but also impairs reliability. Therefore, accurate resonant frequency information is required to operate the power switch in an inductive region that guarantees a ZVS operation. However, the resonant frequency changes according to the temperature of the ship plate, the relative position of the IH coil concerning the ship plate, and the impedance characteristics that vary with the material of the ship plate [9]-[15].

This paper proposes the resonant frequency estimation technique by a real-time impedance estimation algorithm in an input-parallel output-series (IPOS) IH system for heating the ship plate. In addition, the minimum switching frequency is calculated by using the estimated resonant frequency and the snubber capacitance. By limiting the minimum switching frequency of the power switches to the calculated value during power control, the ZVS operation can be ensured in the IPOS IH system. The validity of the proposed technique is experimentally verified using a 4-kW IPOS prototype IH system.

II. IPOS IH SYSTEM

A. IPOS IH System

Since the ship plate that is the load of the IH system has various sizes and materials, the input parallel output series structure is required for a wide heating range. A three-phase transformer is configured to increase the output power by electrically isolating the input AC source and the inverter. The diode rectifier and full-bridge series resonant inverter are composed of one module, as shown in Fig. 1, which can supply a wide output voltage according to the number of modules. The switches of each module operate complementary with a duty ratio of 50% as a pair of S_1, S_4, S_5, S_8, and S_2, S_3, S_6, S_7 shown in Fig. 2 which is the same as the conventional IH inverter. Therefore, the power delivered to the load can be expressed by using first harmonic analysis (FHA) as follows:

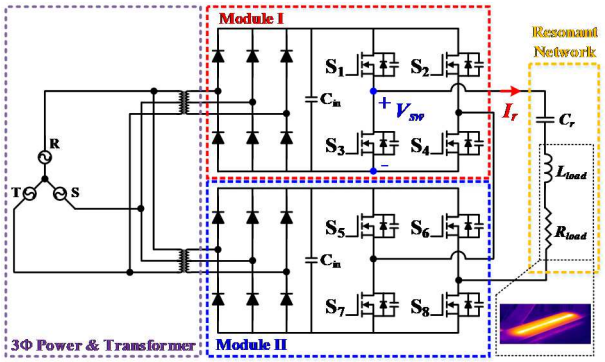

Fig. 1. Circuit diagram of the proposed IPOS IH system (N=2).

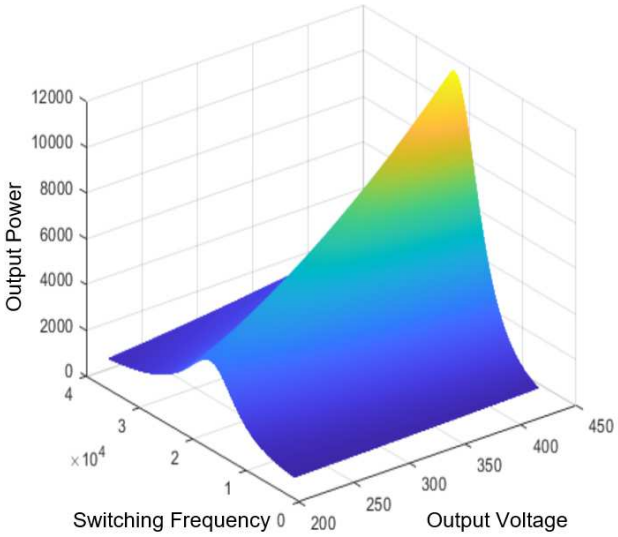

Fig. 2. Output power curve according to the output voltage.

$$P_{res} = \frac{V_{coil}^2}{R_{load}} = \frac{(\frac{2\sqrt{2}}{\pi} \times V_{ac} \times G_V \times N)^2}{R_{load}} \quad (1)$$

where R_{load} and V_{coil} are the load resistance combined with coil and ship plate and the applied voltage to the working IH coil. G_V is the voltage gain of the conventional IH-SRI. V_{in} and N are the input AC voltage and the number of modules of IH-SRI, respectively. By adopting modularization using the IPOS structure, it has a wide output voltage control range and can regulate the output power control by the conventional pulsed frequency modulation (PFM), as shown in Fig. 2. In addition, since each module processes part of the total power in the IPOS IH system, the heating and electrical stress of components in the module are reduced. Therefore, the reliability is high and has the advantage of simple power stage design and system expansion.

B. Operating mode analysis

Fig. 3 is the operating waveform of the IPOS IH system. Operation Modes 4, 5, and 6 are symmetrical with operation Modes 1, 2, and 3. Therefore, modes 1, 2, and 3 shown in Fig. 4 are analyzed in detail. The inductive region operation is assumed.

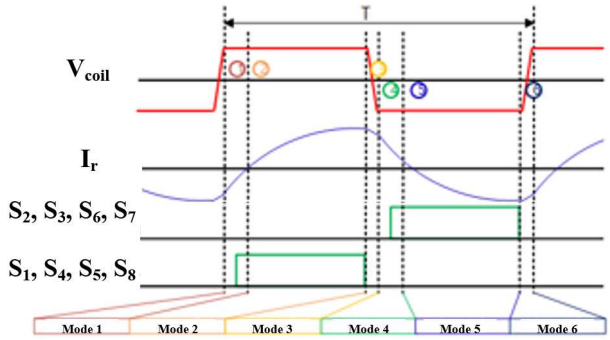

Fig. 3. Operating waveforms of the IPOS IH system.

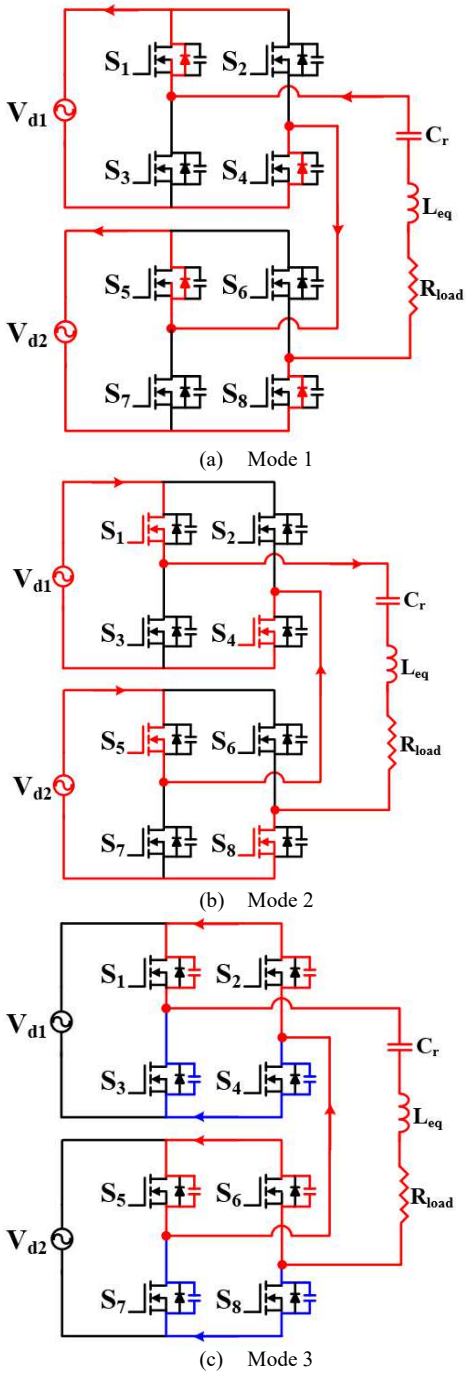

Fig. 4. Current flow diagrams according to the operating modes.

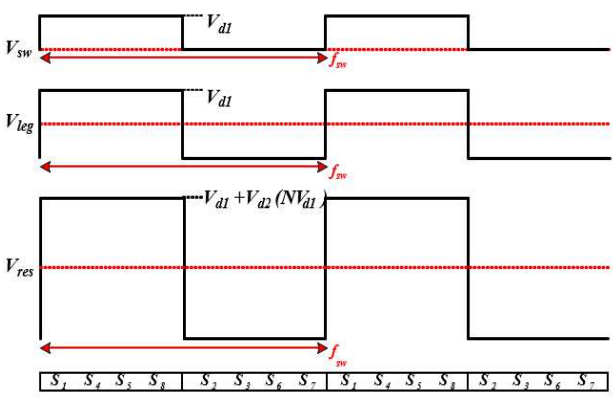

Fig. 5. Voltage waveforms of V_{sw}, V_{leg}, and V_{res}.

In Mode 1, the voltages charged in the output capacitor of the switching devices S_1, S_4, S_5, and S_8 are discharged during the dead time due to the inductive resonance current. After the complete discharge of the output capacitor, it induces the conducting of the reverse diode S_1, S_4, S_5, and S_8. In Mode 2, zero voltage switching (ZVS) is obtained by turning on the switch of S_1, S_4, S_5, and S_8. The sum of the voltage V_{d1} and V_{d2} is applied to the load. In Mode 3, all switches stop operating, and the voltage of the switch's output capacitors are charged due to the resonant current of the load.

III. Impedance Estimation

A. Resonant Frequency Estimation

The resonant inductor and resistance constituting the resonant network change according to the operating frequency and temperature, and even the position of the load relative to the coil. Therefore, the design of the resonant network based on the measurement with the LCR meter brings different results from the actual operation of IH. It can cause operation in the capacitive load region, which degrades the reliability of the IH system due to the inability to control the linear power of the induction heater and hard switching. To solve those problems, real-time impedance estimation is essential to operate the entire IH system in the inductive load region.

Since the resonant capacitor is a design parameter, the load resistance and inductance of the ship plate can be estimated from the impedance of the resonant network in Fig. 1. The impedance can be expressed as follows:

$$Z_{load} = R_{load} + jX_{load} \tag{1}$$

where X_{load} is the load reactance combined with resonant capacitance and coil inductance, respectively. The load resistance and the reactance can be expressed by Ohm's law as follows:

$$\begin{cases} R_{load} = P_{res} \big/ I_{r,rms}^2, P_{res} = P_{sw} \cdot 2N \\ X_{load} = Q_{res} \big/ I_{r,rms}^2, Q_{res} = Q_{sw} \cdot 2N \end{cases} \tag{2}$$

where P_{res} and Q_{res} are the active and reactive power delivered to the resonant network, and $I_{r,rms}$ is the RMS resonant current. P_{res} and Q_{res} can be obtained from the switch voltage and the resonant current from the following relationships:

$$\begin{cases} P_{res} = P_{sw} \cdot 2N, P_{sw} = \dfrac{1}{n}\sum_{k=1}^{n} V_{sw}(k) \cdot I_r(k) \\ Q_{res} = Q_{sw} \cdot 2N, Q_{sw} = \sqrt{S_{sw}^2 - P_{sw}^2} \end{cases} \tag{3}$$

where $V_{sw}(k)$ and $I_r(k)$ are the switch voltage and resonant current sampled at the measurement point, as shown in Fig. 1. P_{sw}, Q_{sw}, and S_{sw} are the active, reactive, and apparent power calculated from the sampled values, respectively. Assuming that the output voltage of each module is the same, the voltage applied to the resonant network is applied twice the switch voltage, as shown in Fig. 5. Therefore, the final value should be multiplied by $2N$ from the values estimated at the switch. From the estimated load reactance, the resonant frequency can be obtained as follows:

$$f_{res} = \frac{1}{2\pi\sqrt{\dfrac{C_r X_{load}}{\omega_{sw}} + \dfrac{1}{\omega_{sw}^2}}} \tag{4}$$

where C_r is the resonant capacitor's capacitance, ω_{sw} is the angular switching frequency.

B. Minimum Switching Frequency Calculation

At the calculated resonant frequency, there is no circulating current to discharge the voltage charged in the snubber when the switch is turned on. Therefore, a minimum switching frequency tracking technique to obtain ZVS capability is proposed. The calculation is based on FHA because the IPOS IH system operates near the resonant frequency.

To discharge the snubber capacitor during dead time, the resonant current should satisfy the condition that is as follows:

$$\begin{cases} I_r(0) \cdot t_d \geq 4(C_{o,es} + C_s) \cdot V_{in,DC} \approx 4C_s \cdot V_{in,DC} \\ I_r(t) = \dfrac{2 \cdot 2N}{\pi |Z_{load}|} V_{in} \sin(\omega_{sw} t - \angle Z_{load}) \end{cases} \tag{5}$$

where t_d and $C_{o,es}$ are the dead time and the output capacitance of the power switch, respectively. C_s is the snubber capacitance, $V_{in,DC}$ is the rectified voltage by the diode rectifier, $\angle Z_{load}$ is the delayed angle by the resonant network's impedance. Equation (5) can be re-expressed as follows:

$$\angle Z_{load} \geq \sin^{-1}\left(\frac{C_s |Z_{load}| \pi}{N \cdot t_d}\right) = A \tag{6}$$

In addition, since the resonant frequency and the quality

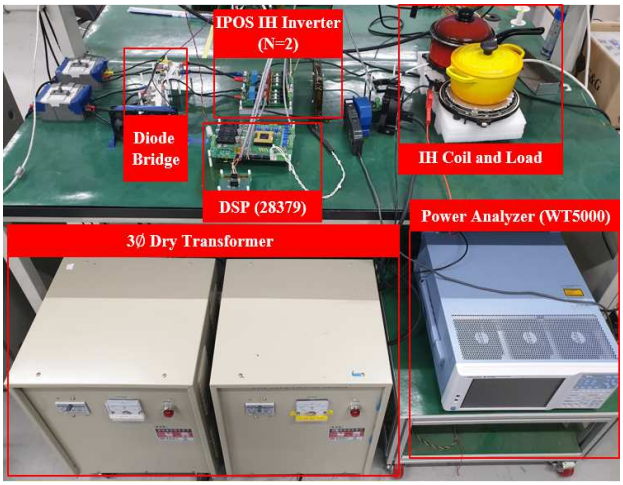

Fig. 6. Experimental setup of 4-kW prototype IPOS IH system.

TABLE I
SPECIFICATIONS OF IPOS IH SYSTEM

Parameter	Value
Input voltage (V_{in})	3Ø 100 V_{rms}
Resonant capacitance	200 nF
Resonant inductance	271-293 uH (offline)
Coil turn number	42 Turn + 21 Turn
Pot material	SUS304 18-10
Snubber capacitor	6.8 nF
Switching frequency	20-40 kHz

factor can be obtained by (2) and (4), $\angle Z_{load}$ can be replaced with (7).

$$\angle Z_{load} = \tan^{-1}\left[Q\left(\frac{\omega_{sw}}{\omega_{res}} - \frac{\omega_{res}}{\omega_{sw}}\right)\right], \quad Q = \frac{\omega_{sw} L_{eq}}{R_{load}} \tag{7}$$

Therefore, the minimum switching frequency to ensure the ZVS capability can be obtained as follows:

$$f_{sw} \geq f_{res} \cdot \frac{\tan(A) + \sqrt{\tan^2(A) + 4Q^2}}{2Q} \tag{8}$$

The controller can secure reliability by ensuring the ZVS operation by limiting the derived minimum switching frequency to the minimum operating frequency of the IPOS IH system.

IV. EXPERIMENTAL RESULTS

To verify the effectiveness of the IPOS IH system and minimum switching frequency tracking method, a

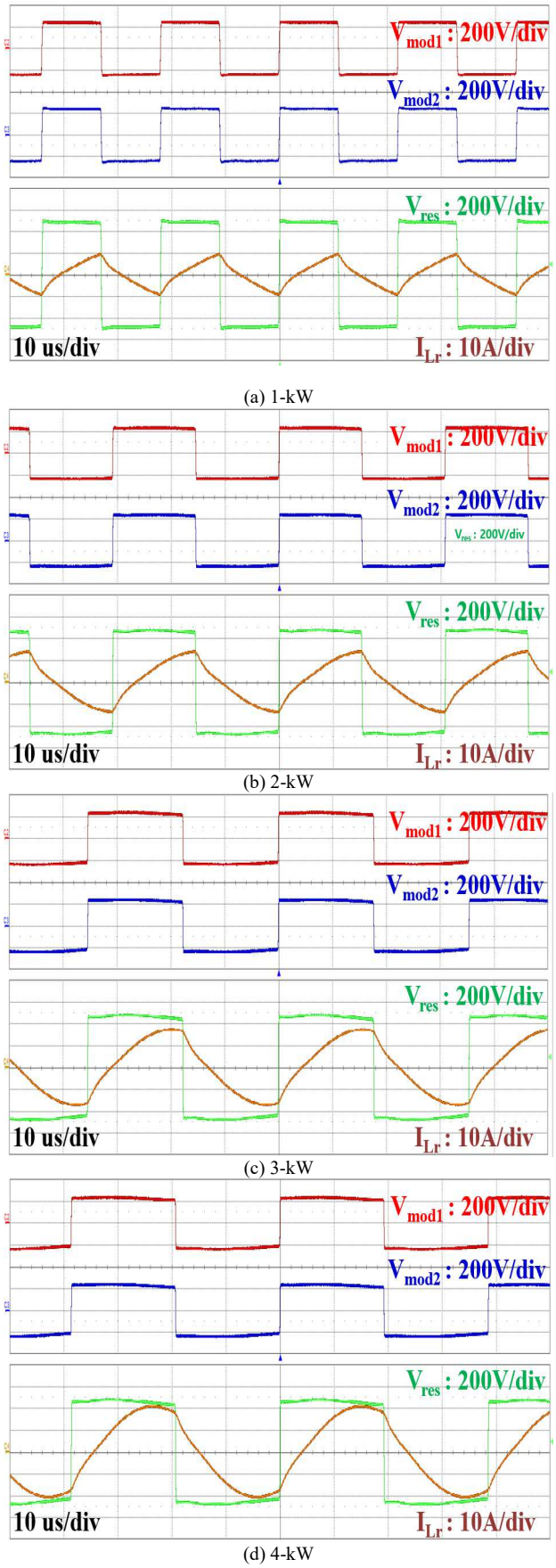

(a) 1-kW

(b) 2-kW

(c) 3-kW

(d) 4-kW

Fig. 7. Steady state waveforms of the IPOS IH system according to the output power.

prototype 4-kW IPOS induction heating system is configured and tested, as shown in Fig. 6. Two induction heating vessels are used assuming a ship's back plate, and 42-turn and 21-turn coils are configured in series. The specifications of the IPOS IH system are shown in Table I. The coil inductance in Table I is measured using IM 3523 (HIOKI).

Fig. 7 shows the steady state waveforms of the IPOS IH system according to output power. As the phases of the drain to source voltages of each module match, the two modules operate in synchronization. The input voltage of the resonant network leads the resonant current under all load conditions, indicating that it operates in the inductive load region. In addition, considering that the voltage input to the resonant network is twice the output voltage of each module, the IPOS IH system has a wide output power range. As the amount of the load increases, the shape of the resonant current approaches a sine wave. It indicates that the operating point is approaching the resonant frequency. In particular, 4-kW is the maximum power that IPOS can output. Its operating point situates at the minimum switching frequency. Since no voltage spike is observed at the drain to source voltage, ZVS capability is ensured at the minimum switching frequency.

Fig. 8 shows the power conversion efficiency curve of the IPOS IH system measured by YOKOGAWA WT5000. It shows a maximum efficiency of 92.4 % and the minimum efficiency of 90.4 %. The efficiency tends to decrease as the output power of the load increases due to an increment in conduction loss. Despite obtaining the ZVS of individual switches, they have high conduction losses due to the configuration of two dry-type transformers and eight switches (IPW65R041CFD, 41) to deliver high power. However, the proposed IPOS IH system has a wide output power range.

V. Conclusions

In this paper, the IPOS IH system for the ship plate is proposed, which can operate at the inductive load region ensuring the ZVS capability. The voltage applied to the resonant network can be amplified according to the number of modules by the IPOS configuration. Therefore, the proposed IH system has a wide output power range, which can correspond to various loads. However, depending on the material, temperature, and position of the coil relative to the load, the IPOS IH system can operate in the capacitive area. It can deteriorate the reliability of the whole system. To solve those problems, a minimum switching frequency tracking algorithm is proposed. It can estimate the impedance of the resonant network using a real-time manner, which ensures the ZVS capability of the IPOS IH system. The effectiveness of the IPOS IH system and the proposed minimum switching frequency tracking technique have been verified by the prototype of a 4-kW IPOS IH system. At the minimum switching frequency point, ZVS capability has been confirmed. The maximum power conversion efficiency is 92.4%, and the minimum efficiency is 90.4 %.

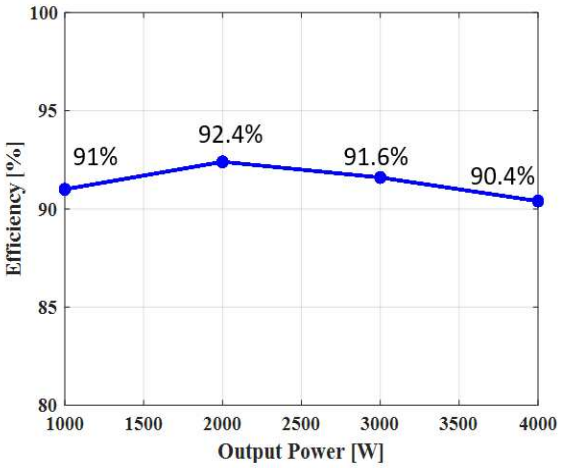

Fig. 8. Power conversion efficiency curve of the IPOS IH system according to the output power.

References

[1] Ó. Jiménez, O. Lucia, I. Urriza, L. A. Barragan, P. Mattavelli and D. Boroyevich, "An FPGA-Based Gain-Scheduled Controller for Resonant Converters Applied to Induction Cooktops," in *IEEE Transactions on Power Electronics*, vol. 29, no. 4, pp. 2143-2152, April 2014.

[2] H. -P. Park and J. -H. Jung, "Load-Adaptive Modulation of a Series-Resonant Inverter for All-Metal Induction Heating Applications," in *IEEE Transactions on Industrial Electronics*, vol. 65, no. 9, pp. 6983-6993, Sept. 2018, doi: 10.1109/TIE.2018.2793270.

[3] M. Kim, H. -P. Park and J. -H. Jung, "Practical Design Methodology of IH and IPT Dual-Functional Apparatus," in *IEEE Transactions on Power Electronics*, vol. 35, no. 9, pp. 8897-8901, Sept. 2020, doi: 10.1109/TPEL.2020.2976054.

[4] M. Kim, H. -P. Park and J. -H. Jung, "Spread Spectrum Technique With Random-Linear Modulation for EMI Mitigation and Audible Noise Elimination in IH Appliances," in *IEEE Transactions on Industrial Electronics*, vol. 69, no. 8, pp. 8589-8593, Aug. 2022, doi: 10.1109/TIE.2021.3102405.

[5] K. -W. Heo, J. Jin and J. -H. Jung, "Maximum Voltage Gain Tracking Algorithm for High-Efficiency of Two-Stage Induction Heating Systems Using Resonant Impedance Estimation," in *IEEE Transactions on Industrial Electronics*, doi: 10.1109/TIE.2022.3225853.

[6] K. -W. Heo, G. -W. Kim and J. -H. Jung, "Vessel Temperature Estimation Method using Equivalent Resistance Difference," *2022 IEEE Applied Power Electronics Conference and Exposition (APEC)*, Houston, TX, USA, 2022, pp. 1329-1332, doi: 10.1109/APEC43599.2022.9773473.

[7] O. Jimenez, O. Lucia, I. Urriza, L. A. Barragan, and D. Navarro, "Design and evaluation of a low-cost high-performance sigma–delta ADC for embedded control systems in induction heating appliances," *IEEE Trans. Ind. Electron*., vol. 61, no. 5, pp. 2601–2611, May 2014.

[8] N. J. Park, D. Y. Lee, and D. S. Hyun, "A power-control scheme with constant switching frequency in class-D inverter for induction-heating jar application," *IEEE Trans. Ind. Electron*., vol. 54, no. 4, pp. 1252–1260, Jun. 2007.

[9] H. Sarnago, Ó. Lucía and J. M. Burdío, "FPGA-Based Resonant Load Identification Technique for Flexible Induction Heating Appliances," in *IEEE Transactions on*

Industrial Electronics, vol. 65, no. 12, pp. 9421-9428, Dec. 2018.

[10] H. Sarnago, O. Lucía and J. M. Burdio, "A Versatile Resonant Tank Identification Methodology for Induction Heating Systems," in *IEEE Transactions on Power Electronics*, vol. 33, no. 3, pp. 1897-1901, March 2018.

[11] Ó. Jiménez, Ó. Lucía, I. Urriza, L. A. Barragán and D. Navarro, "Analysis and Implementation of FPGA-Based Online Parametric Identification Algorithms for Resonant Power Converters," in *IEEE Transactions on Industrial Informatics*, vol. 10, no. 2, pp. 1144-1153, May 2014, doi: 10.1109/TII.2013.2294136.

[12] Ó. Jiménez, Ó. Lucía, L. A. Barragán, D. Navarro, J. I. Artigas and I. Urriza, "FPGA-Based Test-Bench for Resonant Inverter Load Characterization," in *IEEE Transactions on Industrial Informatics*, vol. 9, no. 3, pp. 1645-1654, Aug. 2013, doi: 10.1109/TII.2012.2226184.

[13] Li, Zheng-Feng, Jhih-Cheng Hu, Ming-Shi Huang, Yi-Liang Lin, Chun-Wei Lin, and Yu-Min Meng, "Load Estimation for Induction Heating Cookers Based on Series RLC Natural Resonant Current" in *Energies* 15, no. 4: 1294, 2022.

[14] J. Acero, R. Alonso, J. M. Burdio, L. A. Barragan and D. Puyal, "Analytical equivalent impedance for a planar circular induction heating system," *in IEEE Transactions on Magnetics*, vol. 42, no. 1, pp. 84-86, Jan. 2006, doi: 10.1109/TMAG.2005.854443.

[15] O. Jiménez, L. A. Barragán, D. Navarro, J. I. Artigas, I. Urriza and O. Lucía, "FPGA-based harmonic computation through 1-bit data stream signals from delta-sigma modulators applied to induction heating appliances," *2011 Twenty-Sixth Annual IEEE Applied Power Electronics Conference and Exposition (APEC)*, Fort Worth, TX, USA, 2011, pp. 1776-1781, doi: 10.1109/APEC.2011.5744837.